

Hubbard model with orbital degeneracy and integer or noninteger filling

O. Gunnarsson

Max-Planck-Institut für Festkörperforschung, D-70506 Stuttgart, Germany

(May 3, 2017)

The photoemission spectrum and the specific heat are studied in the Hubbard model of small clusters including orbital degeneracy. We focus on the degeneracy and valence dependence in the limit of a large Coulomb interaction. For integer valence, it is found that the degeneracy increases the width of the photoemission spectrum and it reduces the contribution from the charge degrees of freedom to the specific heat. A deviation from integer valence reduces the width of the photoemission spectrum.

71.10.Fd, 71.20.+h

I. INTRODUCTION

Ni metal provides a typical example of the photoemission spectrum from a relatively strongly correlated system.¹ The width of the Ni 3d band² is reduced by about 25 % compared with one-particle (density functional) calculations.³ As a further signature of many-body effects, the spectrum has a satellite (“6 eV satellite”),² which is displaced by roughly the Coulomb interaction U between two 3d electrons on a Ni atom.⁴ In Ni the many-body effects are primarily due to the localized nature of the 3d orbital. The 3d band has a noninteger occupation (~ 0.6 holes), since the 4s orbital is also partly occupied.

A different example of a rather strongly correlated system is provided by alkali-doped C₆₀ compounds, A₃C₆₀ (A= K, Rb). It is believed that the alkali atoms are almost completely ionized,^{5,6} and the three alkali electrons are therefore donated into the t_{1u} orbital of the C₆₀ molecule, which has a threefold orbital degeneracy. Since in this case essentially only one orbital (t_{1u}) is partly occupied, it has an almost integer occupancy. These systems have slight deviations from stoichiometry, but the occupancy should nevertheless be almost integer. This is in contrast to the noninteger occupancy of the local orbital in many other correlated systems.

For K₃C₆₀ it has not been possible to determine the dispersion of the bands using angular resolved photoemission, due to the presence of orientational disorder and problems related to the angular resolution in relation to the small size of the Brillouin zone. Measurements of the specific heat show, however, that there is no enhancement of the specific heat beyond what would be expected from the electron-phonon interaction.^{7,8} This is quite surprising in view of the expected strong correlation effects in these systems.

The on-site Coulomb energy U between two electrons on the same C₆₀ molecule is large⁹ compared with the one-electron width W of the t_{1u} band, with $U/W \sim 1.5 - 2.5$.^{10,11} For such a large ratio one might have expected the system to be a Mott-Hubbard insulator.¹² We have shown, however, that at half-filling the ratio

of U/W where the transition takes place grows with the orbital degeneracy N of the t_{1u} orbital as \sqrt{N} or somewhat faster.^{10,13} In the large U limit it was shown that an extra electron in a system with otherwise integer occupancy, e.g., half-filled, can move more efficiently if the orbital degeneracy N is large. The reason is that the extra occupancy can move through a hop of any of the electrons on the site with the extra occupancy.^{10,13} In the half-filled case, of the order N electrons can hop to a neighboring site. For a different integer filling than half-filling, this effect is reduced.¹⁴

We observe that in a strongly correlated system hopping is in general reduced compared with the corresponding noninteracting system. Due to the arguments given above, the degeneracy nevertheless enhances the effects of hopping on the Mott transition compared with what might have been expected based on the importance of hopping for the noninteracting system. It is then interesting to ask if this may also happen for other properties.

Here we study photoemission spectroscopy (PES) for the Hubbard model of some finite systems. We show that for these systems and integer occupancy, the width of the PES spectrum is larger than the noninteracting band width W for a large U and $N > 1$, except for filling one and $2N$. These are therefore examples where correlation effects *increase* the band width. The width is reduced as U is reduced or as the valence starts to deviate from an integer and may then become smaller than W . Such systems with noninteger occupation are therefore cases where correlation effects reduce the band width. Systems with noninteger occupancy also develop a satellite which moves roughly linearly with the value of U , while such satellites have very small weights for systems with integer occupancy. We have given a brief discussion of the angular integrated photoemission spectrum for a system with integer valence before.¹⁵

In addition we discuss the contribution to the specific heat from charge degrees of freedom. We show that the orbital degeneracy can reduce this contribution, which may be the reason for the lack of an electronic enhancement of the specific heat in K₃C₆₀.

After giving the formalism (II.A) and presenting some

general arguments (II.B), we show results for the photoemission spectrum for a diatomic molecule (Sec. II.C), a linear chain (Sec. II.D), a six atom cluster (Sec. II.E), a four molecule model of K_3C_{60} (Sec. II.F) and with multiplet effects (Sec. II.G). The specific heat is treated in Sec. III and the results are discussed in Sec. IV.

II. PHOTOEMISSION SPECTRUM

A. Formalism

Below we study multi-band Hubbard models

$$H = \sum_{\langle ij \rangle m \sigma} t_{im,jm'} \psi_{im\sigma}^\dagger \psi_{jm'\sigma} + U \sum_i \sum_{(m\sigma) < (m'\sigma')} n_{im\sigma} n_{im'\sigma'}, \quad (1)$$

where i , m and σ are site, orbital and spin indices, respectively. The orbital index can take N values. The hopping integrals are given by $t_{im,jm'}$ and U is the on-site Coulomb integral. All multiplet effects have been neglected, except in Sec. II.G. The creation operator for an electron with the quantum numbers i , m and σ is given by $\psi_{im\sigma}^\dagger$. We are interested in the spectrum for removing an electron with a given quantum number k

$$\psi_k = \sum_{im\sigma} c(k)_{im\sigma} \psi_{im\sigma}. \quad (2)$$

The spectrum is then given by

$$\rho_k(\varepsilon) = \sum_n |\langle M-1, n | \psi_k | M, 0 \rangle|^2 \delta(\varepsilon - E_0(M) + E_n(M-1)), \quad (3)$$

where $|M, 0\rangle$ is the initial ground-state with M electrons and $|M-1, n\rangle$ is an excited final state. The corresponding energies are $E_0(M)$ and $E_n(M-1)$, respectively. We use Lanczos method to calculate the ground-state and the spectrum.¹⁶ In most, but not all, cases we assume that the hopping matrix elements are “diagonal” in m and m'

$$t_{im,jm'} = \begin{cases} t \delta_{mm'}, & \text{if } i \text{ and } j \text{ nearest neighbors;} \\ 0, & \text{otherwise.} \end{cases} \quad (4)$$

Here we assume t to be negative.

B. General considerations

We first address the hopping of an electron or a hole in a system which otherwise has integer occupancy. We consider the large U -limit. We construct a Neel state $|0\rangle$ with N electrons of the same spin per site. We now add an extra electron to site 1 and obtain the state

$$|1\rangle = \psi_{11\downarrow}^\dagger |0\rangle. \quad (5)$$

The extra occupancy on site 1 can now hop to the neighboring sites i without any extra cost in Coulomb energy. We can form a state where the extra occupancy is on the neighboring site i

$$|i\rangle = \frac{1}{\sqrt{N}} \psi_{11\downarrow}^\dagger \sum_m \psi_{im\uparrow}^\dagger \psi_{1m\uparrow} |0\rangle. \quad (6)$$

We have here taken into account that any of the N spin up electrons on site 1 can hop to site i , as is illustrated in Fig. 1a. Assuming hopping matrix elements of the form (4), we obtain the matrix element¹⁰

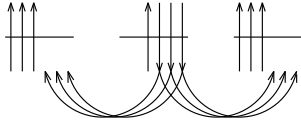
$$\langle i | H | 1 \rangle = \sqrt{N} t, \quad (7)$$

where t is the one-particle matrix element. Thus the hopping matrix element has been enhanced by a factor of \sqrt{N} . In this argument we have assumed that the electron hops against a background of a classical Neel state. For certain systems, we have constructed states where the hopping energy of the extra electron or hole is more negative.¹³ The hopping may therefore be enhanced by a somewhat larger factor than \sqrt{N} in the large U case for certain systems.¹³

In Fig. 1b we show schematically a doped system. The electron added to the central site in an inverse photoemission process sees a neighboring site which also has an extra electron. This additional electron blocks one hopping channel. In the large U case the effect is, however, much more dramatic, since hopping to a site with an extra electron is then completely suppressed.

The doping of the system has a strong effect on the satellite structure. Let us consider the large U limit for a system with the average number $K+x$ electrons per site. Then a fraction $1-x$ of the sites have K electrons and a fraction x have $K+1$ electrons. If an electron is now removed from a site with K electrons, there is a strong coupling to final states with $K-1$ electrons on that site. The energy of such a state is about U higher than for a final state where all sites have K or $K+1$ electrons. The result is a satellite at about the energy U below the main peak.¹ The weight of this satellite is reduced as $1-x$ is reduced.

a)



b)

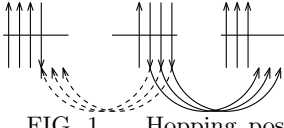


FIG. 1. Hopping possibilities in the undoped (a) and doped (b) system. In the undoped system the extra occupancy can hop in N ways to neighboring sites. In the doped case hopping to other sites with an extra occupancy is blocked if the Coulomb interaction is large.

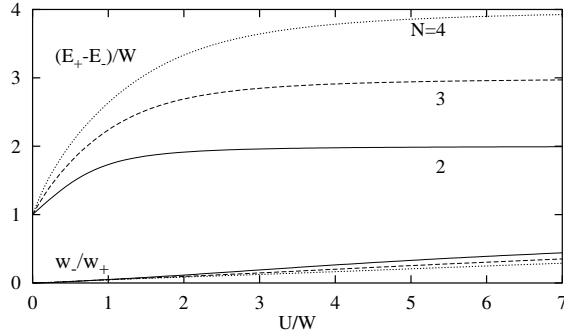


FIG. 2. Photoemission from a diatomic molecule with orbital degeneracy N and an integer (N) number of electrons per site at the “Brillouin zone centre” (+) and “boundary” (-). The dispersion (band width) $E_+ - E_-$ and the ratio w_-/w_+ of the weights of the two peaks are shown. W is the splitting (band width) between the bonding and antibonding levels for the noninteracting system. The figure illustrates how the dispersion increases with the Coulomb interaction U and becomes proportional to N for large U .

C. Diatomic molecule

We first consider the case of a diatomic molecule with only two sites and with two electrons. This model has been treated by Harris and Lange¹⁷ in the absence of orbital degeneracy. An electron is removed from a bonding or an antibonding orbital for the orbital quantum number m and $\sigma = \uparrow$,

$$\psi_{\pm m\uparrow} = \frac{1}{\sqrt{2}}(\psi_{1m\uparrow} \pm \psi_{2m\uparrow}), \quad (8)$$

and the result is averaged over m . For the case $N = 1$ the problem can easily be solved analytically, and we find

$$\rho_{\pm}(\varepsilon) = \alpha_{\pm} \delta(\varepsilon - E_0(2) \pm t), \quad (9)$$

where $\alpha_{\pm} = (1 + x^2 \pm \sqrt{1 + x^2})/[2(1 + x^2)]$ and $E_0(2) = 2|t|(x - \sqrt{1 + x^2})$, with $x = U/(2|t|)$. For $U \rightarrow 0$ the weight α_- of the antibonding state goes to zero, and for $U = 0$ the spectrum has only one peak. For $U > 0$ the separation between the peaks for ρ_+ and ρ_- is $2|t| = W$, where W is the one-particle band width. Thus the width of the angular integrated PES spectrum is the full one-particle band width W ,¹⁸ and not the width of the occupied part. We can think of this width as a dispersional width, since the two peaks in the angular integrated spectrum correspond to two different values of k . In the solid, these k values correspond to the Brillouin zone centre and boundary, respectively.

We next consider the two-site model for an orbital degeneracy $N > 1$. We first consider the case with $2N$ electrons, i.e., an integer number of electrons per site. For the model (Eq.(4)) of the hopping used here, the one-particle band width remains $W = 2|t|$ independently of N . Fig. 2 shows the splitting $E_+ - E_-$ of the peaks in $\rho_{\pm}(\varepsilon)$ as a function of U for different values of N . The splitting grows with U from its noninteracting value W to its large U -limit NW . In the large U -limit the weights w_{\pm} of the peaks in ρ_{\pm} become equal. As shown in the Fig. 2 this limit is reached quite slowly as U/W grows. In addition to these peaks, there are satellites at about $2U$ lower energy. These satellites have, however, very small weights. The reason for the large splitting between the bonding and antibonding peak is the degeneracy N . In the case of a two-site model it can be shown¹³ that the hopping is enhanced by a factor N instead of the factor \sqrt{N} in the simple argument above.

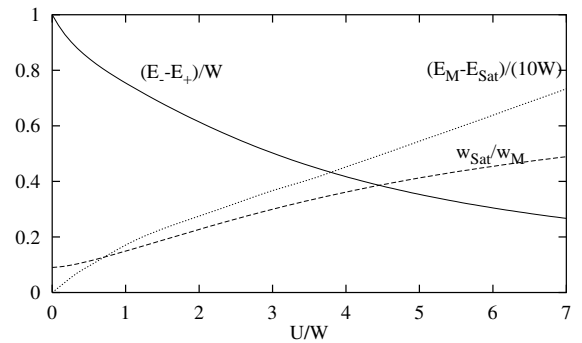


FIG. 3. Photoemission from a diatomic molecule with orbital degeneracy $N = 2$ and a noninteger (2.5) number of electrons per site. The dispersion (band width) $E_- - E_+$, the satellite to main peak splitting $E_M - E_{Sat}$ and the ratio of the satellite and main peak weights w_{Sat}/w_M are shown. W is the splitting (band width) between the bonding and antibonding levels for the noninteracting system. The figure illustrates how the dispersion is reduced as the Coulomb interaction U is increased.

We next consider the two-site model with $2N + 1$ electrons, i.e., a noninteger number ($N + \frac{1}{2}$) of electrons per

site. In the large U -limit, the ground-state now has $N+1$ electrons on one site and N electrons on the other site. If an electron is removed from the site with $N+1$ electrons in a photoemission process, the system is left with N electrons on each site. As discussed above, hopping is now completely suppressed in the large U limit, and we expect a negligible dispersion in the final state. If, on the other hand, the electron is removed from the site with N electrons, the result is a satellite, as discussed above. These results are illustrated in Fig. 3 for the case $N=2$. For $U=0$ the electron can be removed from a bonding ($k=+$) or antibonding ($k=-$) orbital, giving a dispersion W . In this limit ρ_{\pm} have just one peak each. As U is increased, the dispersion (separation between the main peaks E_{\pm}) decreases and goes to zero for $U \rightarrow \infty$. At the same time satellites develop at an energy about U below the main peaks. The weights of these satellites approach the weight of the main peaks in the large U -limit. Since there are several satellites with slightly different energies, we have calculated the average energy of the satellites in the two spectra ρ_{\pm} . The splitting between the main peak and the average satellite position was then averaged for the two spectra using the total satellite weight in each spectra as a weight factor.

For the diatomic molecule with $N > 1$ we thus find that the dispersive band width increases with U for integer occupancy (N) but decreases with U for half integer occupancy ($N+1/2$) relatively to the noninteracting width W .

D. Linear chain

The one-dimensional Hubbard model has been studied very extensively in the literature.¹⁹ We first consider a linear chain with six sites, periodic boundary conditions and $N=1$. Fig. 4a shows the angular resolved spectrum for different values of k . The figure illustrates that there is a substantial dispersion as in the diatomic molecule. Thus the width of the occupied part of the spectrum is only $0.25W$ for noninteracting electrons, but for interacting electrons ($U/W=30$) the width is about W ¹⁸ for $N=1$. The spectrum is more complicated than for the diatomic molecule, having several peaks for each k -value. In the large U -limit, appropriate here, the spectrum can be interpreted in terms of holons and spinons.¹⁹

Fig. 4b shows the angular resolved spectrum for $N=2$. The spectrum has more structures than for $N=1$ (Fig. 4a) but the gross features are very similar. A major difference is, however, that the energy scale is about a factor of two larger. Thus the width of the spectrum is now almost twice (~ 1.8) the one-particle band width W . This increased width is not due to the creation of new satellites with a large binding energy, but due to a rather uniform expansion of the energy scale for all the features present for $N=1$. This is illustrated by the centre of gravity which has a stronger k -dependence

for $N=2$. Thus we may think of the increased band width as to a large extent being due to an increased dispersion. In this sense the situation is rather similar to the case of the diatomic molecule considered before.

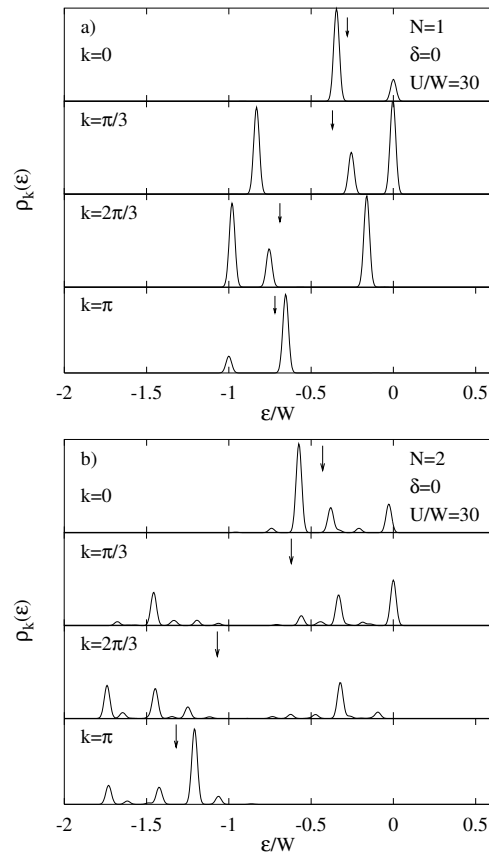


FIG. 4. Photoemission spectrum of a six atom linear chain with six electrons (integer occupancy=1, doping $\delta=0$) as a function of k and ϵ . The orbital degeneracy is $N=1$ in a) and $N=2$ in b). The one-particle band width is W and $U/W=30$ is very large. The arrows show the centre of gravity of the main part of the spectrum, excluding the contribution from any satellite at about $\epsilon/W \sim -30$ or lower. For plotting reasons a Gaussian broadening of $0.04W$ (full width half maximum) has been introduced. The energy zero is given by the leading peak. Comparison of a) and b) shows that the energy scale of the spectrum has been expanded by almost a factor of two due to the degeneracy.

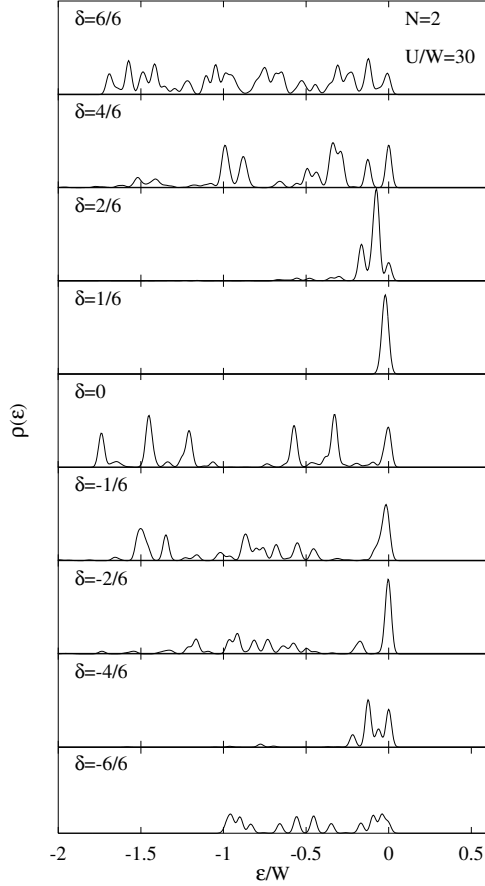


FIG. 5. Photoemission spectrum of a six atom linear chain as a function of doping δ , where the number of electrons is $(2+\delta)6$. The orbital degeneracy is $N = 2$ and the one-particle band width is W . The figure illustrates how the width of the spectrum is reduced when δ is changed from $4/6$ to $1/6$ or from 0 to $-4/6$. Observe the dramatic difference between doping $\delta = 1/6$ and $\delta = -1/6$. For integer fillings 1 ($\delta = -6/6$) and 2 ($\delta = 0$) and 3 ($\delta = 6/6$) the spectrum is broad.

We next consider the results for a doped system with $(2 + \delta)6$ electrons and $N = 2$. The angular integrated spectra are shown in Fig. 5. As the doping δ becomes increasingly negative, the spectrum becomes narrower. The same tendency is seen when δ is positive and reduced from $4/6$ to $1/6$. For $\delta = 1/6$, the width of the spectrum is essentially zero (apart from an artificial broadening used for plotting reasons). The explanation is the same as for the diatomic molecule. With doping $\delta = 1/6$ the system has two electrons on five sites and three electrons on one site. To obtain a contribution to the main peak the electron must be removed from the site with three electrons. We then obtain a final state with two electrons on each site. Since hopping then costs the energy U , it is strongly suppressed and the width of the spectrum goes to zero. This general tendency also shows up for intermediate dopings, and it reflects the reduced hopping possibilities for the photoemission hole if it is

surrounded by other holes. It is instructive to notice the asymmetry between doping $\delta = 1/6$ and $\delta = -1/6$. In the first case hopping is completely suppressed in the final states corresponding to the leading peaks, as discussed above. In the case $\delta = -1/6$, on the other hand, the probability that the photoemission hole can hop to a neighboring site would only be reduced from 1 to $5/6$, if the occupancies were spatially uncorrelated, and there is a small reduction in the width. In inverse photoemission the situation is reversed, with a large reduction in the width for $\delta = -1/6$ and a small reduction for $\delta = 1/6$.

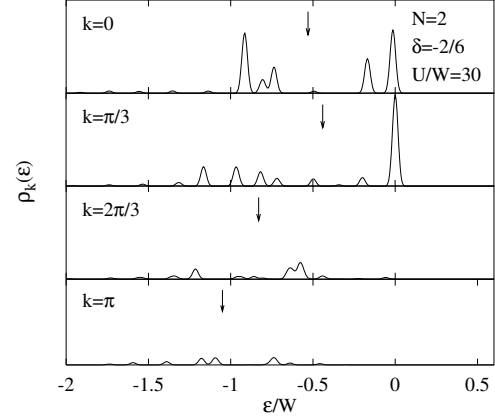


FIG. 6. The same as in Fig. 4b but for the doping $\delta = -2/6$ (ten electrons). Comparison with $\delta = 0$ (Fig. 4b) shows that the spectra with the lowest centre of gravity ($k = 2\pi/3, \pi$) have lost weight and that the centre of gravity of each spectra tends to move upwards.

To see how this happens in more detail, we show in Fig. 6 the angular resolved spectrum for $\delta = -2/6$. Compared with the $\delta = 0$ results in Fig. 4b, the spectrum for $k = \pi$ has a small weight. Since the centre of gravity of this spectrum is low, the reduction of its weight leads to a reduced width of the angular integrated spectrum. The same applies to a smaller extent to the $k = 2\pi/3$ spectrum. Furthermore, the centres of gravity of the spectra for $k = \pi/3$ and $2\pi/3$ have moved upwards. This can be viewed as a reduction of the dispersion, and it also contributes to the reduced width of the angular integrated spectrum. This upward movement of the centre of gravity is partly due to an upward movement of certain peaks and partly due to a reduced weight of peaks with large binding energies.

Fig. 7 shows the angular resolved spectrum for a positive doping. In this case the centres of gravity have moved up strongly for $k = 0, \pi/3$ and $2\pi/3$. In addition, the spectrum for $k = \pi$ now has a negligible weight, while for $\delta = 0$ it contributed substantially to the width of the spectrum due to its low centre of gravity. In this case the reduction of the width of the angular integrated spectrum is, however, mainly due to a reduced dispersion, while the situation is less well-defined in Fig. 6.

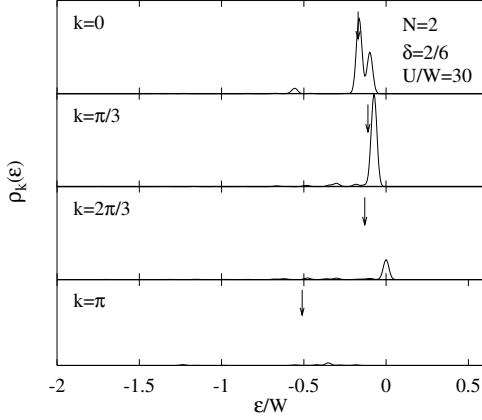


FIG. 7. The same as in Fig. 4b but for the doping $\delta = 2/6$ (fourteen electrons). Comparison with $\delta = 0$ (Fig. 4b) shows that the centres of gravity of the spectra for $k = 0, \pi/3$ and $2\pi/3$ have moved upwards, strongly reducing the dispersion. Furthermore, the spectrum with the lowest centre of gravity ($k = 2\pi/3, \pi$) has lost most of its weight.

It is also interesting to consider integer filling away from half-filling. The arguments in Sec. II.B can be straightforwardly generalized to any integer filling.¹⁴ If the filling is $K \leq N$, there are K electrons which can fill a hole on the site where a hole was created in the photoemission process. If the filling is $K > N$ there are $2N - (K - 1)$ holes which can be filled on the site where a hole was created in the photoemission process. Above we found that the width of the photoemission spectrum grows linearly with the number of hopping possibilities for a linear chain. For the fillings $K = 1$ and $K = 3$ this suggests the band widths W and $2W$, respectively, for $N = 2$. These results are confirmed by the explicit calculations shown in Fig. 5. In inverse photoemission we expect $K + 1$ hopping possibilities for $K < N$ and $2N - K$ hopping possibilities for $K \geq N$.

Up to now the linear chain has been discussed in the limit of $U/W \gg 1$. Fig. 8 illustrates the validity of these conclusions for intermediate values of U/W . The figure shows the width

$$\mathcal{W} = 2\sqrt{S_2 - S_1^2}, \quad (10)$$

where S_i is the i th moment of the spectrum. Also shown is the centre of gravity relative to the leading peak. The figure illustrates that the spectrum is broadened even for small values of U . For $U/W > 1$ the degeneracy furthermore becomes important and the width is substantially larger for $N = 2$ than $N = 1$.

Fig. 9 shows the spectra for $U/W = 1.5$ for $N = 1$ (a) and $N = 2$ (b). The figure illustrates that a substantial part of the large width in the $N = 2$ case comes from the spectra for $k = 2\pi/3$ and $k = \pi$, which have small weights but structures at large binding energies. Such contributions would probably be very hard to detect experimentally. There is, however, also a downward shift

in the spectra for $k = 0$ and $k = \pi/3$.

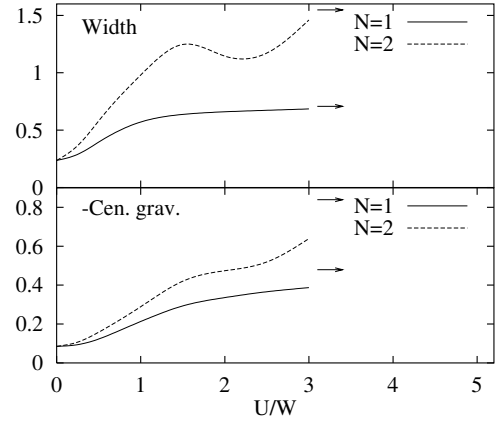


FIG. 8. Width and the negative of the centre of gravity (relative to the leading peak) of the spectrum for $N = 1$ and $N = 2$ as a function of U/W . The horizontal arrows show the results for $U/W = 30$. The figure illustrates how the effects discussed remain important down to $U/W \sim 1$.

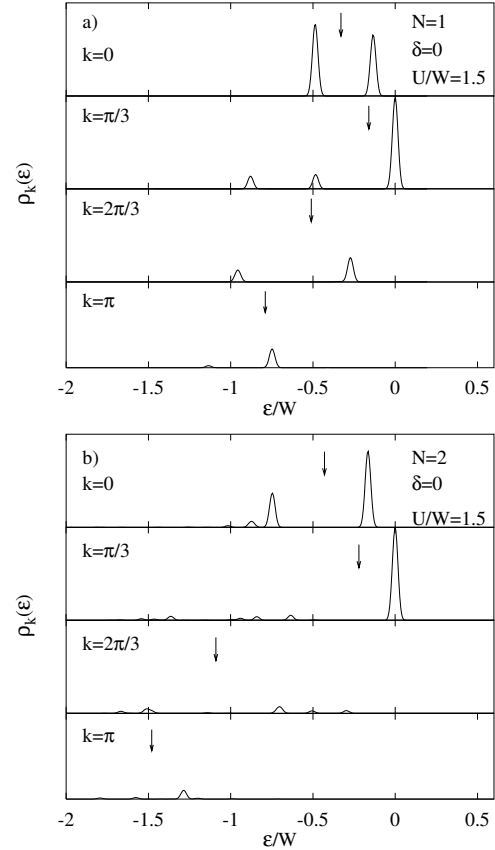


FIG. 9. Same as in Fig. 4 but for $U/W = 1.5$. The figure illustrates that the effects in Fig. 4 are substantially reduced at intermediate values of U , but that some effects still remain.

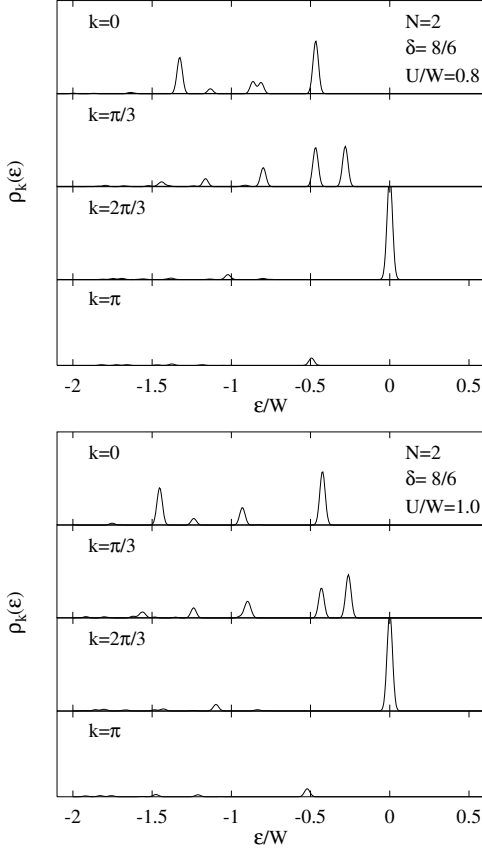


FIG. 10. The same as in Fig. 4b but for doping $\delta = 8/6$ (0.67 holes per site) and $U/W = 0.8$ (a) and $U/W = 1.0$ (b). These parameters may be typical for Ni metal. Comparison of (a) and (b) illustrates how the peaks above $\sim -W/2$ move upwards as U is increased (“band narrowing”) while the peaks below $\sim -W/2$ move downwards (“satellites”). For $U = 0$ the width of the photoemission spectrum is $0.75W$.

Finally we consider parameters which may be considered as representative for Ni metal. Thus we have chosen $U/W = 0.8$ (Fig. 10a) and $U/W = 1.0$ (Fig. 10b) and the doping $\delta = 8/6$, which corresponds to 0.67 holes per site. According to Auger measurements, U/W for Ni is close to but slightly smaller than one.²⁴ The number of $3d$ -holes in Ni is about 0.6. As discussed earlier, because of the noninteger number of electrons per sites, we expect satellites that move down in energy with U . To distinguish between these types of satellites and the “main” band, we have performed the calculation for two values of U . In Fig. 10 the peaks below about $-W/2$ move downwards as U is increased, while the peaks above $-W/2$ move upwards. Although U/W is not large in this case, we can therefore nevertheless identify the peaks below $-W/2$ as satellites. This means that the main band has only a width of about $0.45W$. This should be compared with the width $0.75W$ of the occupied part of the band for $U = 0$. This means that the band width has been reduced by about 40 %. This is a bit larger than the ex-

perimental result (25%), but it illustrates that the model gives a qualitatively correct band width, in spite of its extreme simplicity.

To understand the band narrowing, we observe that for a site with two electrons the probability that a given neighboring site also has two electrons would be $1/6$ if the sites with two electrons were uncorrelated. There is then one hopping possibility for the hole to such a site, while hopping to all other site costs the energy U . This would then suggest a reduction of the band width to $W/6$. Actual calculations for $U/W = 30$ give reduction by a factor somewhat smaller than five. The much less dramatic reduction of the band width in Fig. 10 is due to the value of U being intermediate.

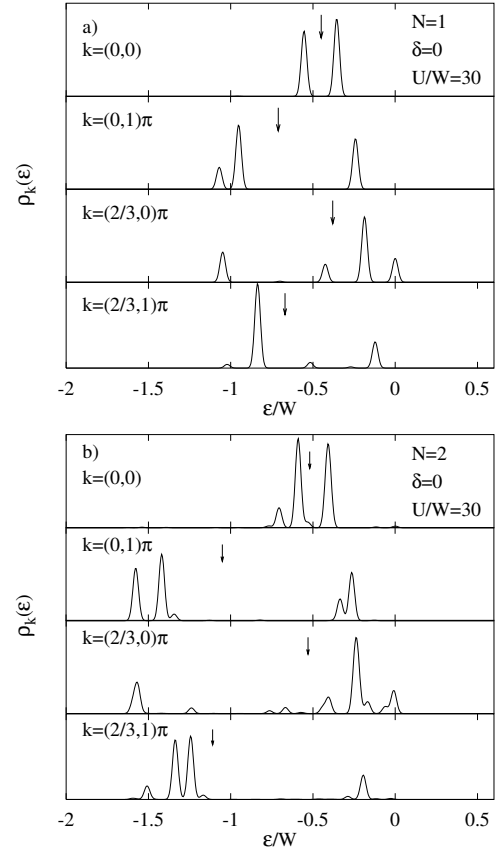


FIG. 11. Photoemission spectrum of a cluster with six atoms in a rectangular arrangement (2×3) with six electrons (integer occupancy) and $U/W = 30$ for $N = 1$ a) and $N = 2$ b). The arrows show the centre of gravity of the main part of the spectrum, excluding any satellite at $\varepsilon/W \sim -30$ or lower. Comparison of a) and b) shows how the energy scale has been expanded by about a factor of 1.5 for $N = 2$ compared with $N = 1$.

E. Six atom "rectangular" cluster

As an further example we study a cluster with six atoms arranged in a rectangle with three times two sites, using periodic boundary conditions. Fig. 11a shows the spectrum for the orbital degeneracy $N = 1$. In this case the width of the photoemission spectrum is even larger than the one-particle band width W . The reason¹³ is the frustration in the six atom cluster due to the periodic boundary conditions. Because of this, the one-particle band width $W = 5|t|$ is smaller than one might have expected ($6|t|$) from the hopping integral and the number of nearest neighbors ($=3$). The frustration effect on the many-body spectrum for a large U/W is smaller, giving a width of the spectrum of about $5.75|t| = 1.15W$ already for $N = 1$. The width of the angular integrated spectrum is to a substantial amount due to the dispersion.

Fig. 11b shows the spectrum for $N = 2$. The spectrum shows large similarities with the case $N = 1$ (Fig. 11a), except that the energy scale is larger by a factor of about 1.5. This behavior lies in between \sqrt{N} and N and has been discussed in Ref. 13. Fig. 11 illustrates that the increase of the width of the spectrum with N is not limited to the linear chain but a general phenomenon.

F. A_3C_{60} ($A = K, Rb$)

The photoemission from A_3C_{60} ($A=K, Rb$) is interesting, since the experimental width of the spectrum is about 1.5 eV,²⁰ while the occupied width of the one-particle spectrum is only of the order of 0.3 eV.⁶ As discussed in the introduction, however, the experimental spectrum is angular resolved, and it is not known if this large width is due to dispersion or satellites. We have considered multi-band Hubbard model in Eq. (1) to describe the $C_{60} t_{1u}$ level with degeneracy three. The hopping matrix elements are obtained from a tight-binding theory,^{22,6,23} which takes the orientational disorder in A_3C_{60} into account. We use parameters which give a one-particle full band width $W = 0.6$ eV. The angular integrated photoemission spectrum is shown in Fig. 12. The total width of the spectrum is about 1.5 eV. This width is larger than $\sqrt{N}W \sim 1$ eV. This may be due to the width growing somewhat faster than \sqrt{N} and to the system being frustrated because of the fcc lattice.

The calculated width of the spectrum is of the same order as observed experimentally. In contrast to the experimental spectrum there is, however, no weight in the range -0.3 to -0.7 eV, while the experimental spectrum is smoothly reduced with increasing binding energy. The calculated spectrum also has much too much weight at small binding energies. The spectrum in Fig. 12 can therefore not explain experiment. The main contribution to the broad experimental spectrum is therefore probably from phonon and plasmon satellites, as suggested earlier.²¹ The degeneracy mechanism discussed

here should, however, make some contribution to the weight at large binding energies.¹⁵

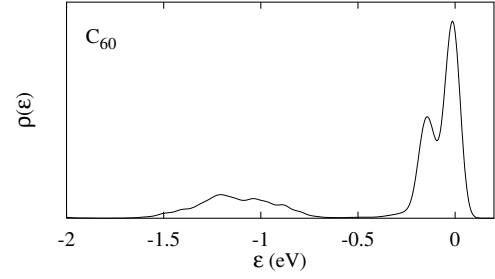


FIG. 12. Photoemission spectrum from a model of four C_{60} molecules for $U = 1.3$ eV. The figure illustrates that apart from the main peak there is additional weight at about -1 to -1.5 eV. This weight does not move as U is increased and it is related to the three-fold orbital degeneracy.

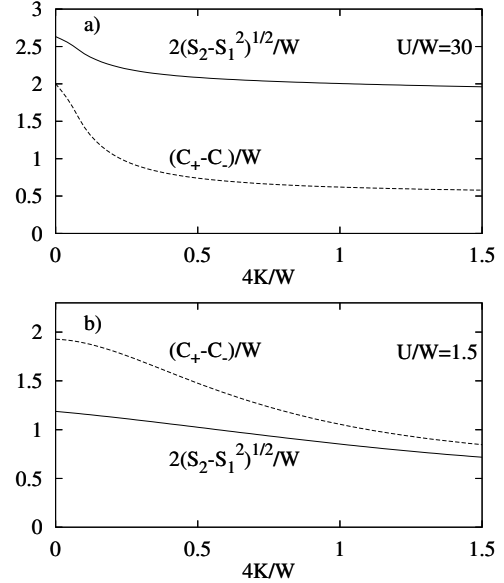


FIG. 13. The dispersion $C_+ - C_-$ and the width $2\sqrt{S_2 - S_1^2}$ of the photoemission spectrum as a function of the multiplet splitting $4K$ for a two-site system, where K is the multiplet integral. C_{\pm} is the centre of gravity for $k = \pm$. A large ($U/W = 30$) and an intermediate ($U/W = 1.5$) value of U were considered.

G. Multiplet effects

An interesting question is how these results are influenced by multiplet effects. If a site with an extra electron or hole is in a given multiplet state, the hopping of the extra occupancy to a neighboring site with a similar energy may be restricted, because the multiplet effects lift degeneracies.

Here we consider a model, where the multiplet effects are described by the exchange integral K between two different orbitals and the difference $\delta U \equiv U_{xx} - U_{xy}$ between the direct Coulomb integral for equal and unequal orbitals. Here we use $\delta U = 2K$. Thus we add the multiplet terms

$$\begin{aligned}
H_U = & \frac{2}{3}\delta U \sum_{im} n_{im\uparrow} n_{im\downarrow} - \frac{1}{3}\delta U \sum_{i\sigma\sigma'} \sum_{m < m'} n_{i\sigma m} n_{i\sigma' m'} \\
& + \frac{1}{2}K \sum_{i\sigma\sigma'} \sum_{m \neq m'} \psi_{i\sigma m}^\dagger \psi_{i\sigma' m'}^\dagger \psi_{i\sigma' m} \psi_{i\sigma m'} \\
& + \frac{1}{2}K \sum_{i\sigma} \sum_{m \neq m'} \psi_{i\sigma m}^\dagger \psi_{i-\sigma m}^\dagger \psi_{i-\sigma m'} \psi_{i\sigma m'}
\end{aligned} \quad (11)$$

to the Hamiltonian in Eq. (1). This part of the Hamiltonian has multiplets with the energies 0, $2K$ and $4K$ relative to the lowest multiplet, i.e., a splitting of $4K$.

We consider a system with two sites, the orbital degeneracy $N = 2$ and four electrons, i.e., integer occupancy. Fig. 13 shows results for the width $2\sqrt{S_2 - S_1^2}$ and the separation ($C_+ - C_-$) in the centres of gravity of the spectrum, where S_i is the i th moment. For a large U (Fig. 13a) the width of the spectrum is gradually reduced with the multiplet splitting as expected, but the reduction is moderate. The "dispersion" measured through $C_+ - C_-$ drops is reduced much more. The reason for this drop is a change in the character of the spectrum. For $K = 0$ the spectra for $k = \pm$ have essentially just one peak each. As K is increased, new satellites are formed on the energy scale W (not K !), which lead to rapid reduction in the difference $C_+ - C_-$, without changing the total width of the spectrum drastically. The creation of new satellites are related to changes in the ground-state wave function. Due to the integer occupancy in the ground-state, the hopping energy is very small, and the energy scale over which the multiplet effects become important is very small. Fig. 13b shows results for an intermediate value of U . In this case the hopping in the initial state is more important, and a small value of K has a small influence on the ground-state. Both $C_+ - C_-$ and $2\sqrt{S_2 - S_1^2}$ are now reduced with $4K$ at a much slower rate. Due to the smaller value of U , however, both quantities are smaller for $K = 0$ than in Fig. 13a. The results above suggest that multiplet couplings reduce the effects discussed in this paper, but that these effects are still present for intermediate multiplet splittings.

III. SPECIFIC HEAT

If the dispersion of the states is indeed increased due to the degeneracy, this should also show up as a reduction in the specific heat. We thus consider the specific heat

$$c_v = \frac{dE(T)}{dT}, \quad (12)$$

where $E(T)$ is the energy of the system as a function of the temperature T . To perform the calculation at finite T , we use a technique developed by Jaklic and Prelovsek,²⁵ and based on the Lanczos method. In this technique a certain number of states N_0 are chosen randomly, and for each state $|n\rangle$ the appropriate expectation values $\langle n | \exp(-H/T) | n \rangle$ and $\langle n | \exp(-H/T) H | n \rangle$ are calculated using the Lanczos method. We here use the grand canonical ensemble, i.e., the number of electrons is not fixed. In this approach the specific heat is independent of the degeneracy for noninteracting electrons, as it should. The use of the canonical ensemble leads to a moderate degeneracy dependence even for $U = 0$, due to the finite size of the system and the change of the number of electrons with degeneracy, i.e., the system being closer to infinite for a larger N .

We consider the Hubbard model for a six-atom cluster with the atoms arranged in a 3×2 rectangle, as above. The hopping integrals in Eq. (4) are used. In the large U -limit the total energy at half-filling for a system with M sites and the orbital degeneracy N is

$$E(T = 0) = \frac{1}{2}MN(N - 1)U. \quad (13)$$

Here we have neglected small terms of the order $-t^2/U$. For a very large temperature we obtain

$$E(T = \infty) = \left(\frac{1}{2}\right)^2 MN(2N - 1)U. \quad (14)$$

The energy increase per electron is then

$$\frac{1}{MN} [E(T = \infty) - E(T = 0)] = \frac{1}{4}U, \quad (15)$$

i.e., independent of the degeneracy N . Integrating $c_v/(MN)$ over all temperatures should then give a quantity which is independent of N for large U . In this limit, we therefore expect the specific heat to be reduced with N but to remain appreciable over a correspondingly larger temperature range.

We may think of the contributions to the specific heat as resulting from the excitation of spin and charge degrees of freedom. Due to its finite size, the system has a band gap even for small values of U . For $U/W = 1.5$ and $N = 1$ the gap is $E_g = 0.76W$ and for $N = 2$ we find $E_g = 0.45W$. For T much smaller than the band gap, charge degrees of freedom are not excited, and only spin excitations contribute to the specific heat. Fig. 14 shows the spin correlation function

$$\frac{1}{4NM} \sum_{\langle i,j \rangle m} \langle \sigma_{im}^z \sigma_{jm}^z \rangle, \quad (16)$$

where the summation is over nearest neighbors and σ_{im}^z is the Pauli spin matrix σ^z for orbital m on site i . The figure illustrates that the spins become uncorrelated over an energy scale of about a few tenths of W . This energy

scale is smaller than the band gap and for the corresponding temperatures the spin excitations should dominate the specific heat. The specific heat is also shown in Fig. 14. The present system may be too small to describe the spin degrees of freedom of a large system, since at low temperatures only a very small number of states contribute to the specific heat, and since we do not know if these few states are representative of a larger system. Thus the sharp peak in c_v for small T 's may be a defect of the small size of the system. We are interested in metallic systems, i.e., systems where the band gap goes to zero with increasing system size. For these systems the charge degrees of freedom should become increasingly important for low temperatures as the size of the system grows. Because of this and because of the uncertainty in the contribution from the spin degrees of freedom we here concentrate on the charge degrees of freedom, dominating for $T \gtrsim 0.2W$ for the six atom cluster.

For low temperatures in this range, the specific heat is smaller for $N = 2$ than for $N = 1$, in agreement with the expectations above. The specific heat decreases more slowly with T for $N = 2$, remaining appreciable up to larger values of T . This is required to satisfy Eq. (16). Finally we remark that although we have not discussed the spin degrees of freedom further, these degrees give an important contribution for many strongly correlated systems.

IV. CONCLUDING REMARKS

We have studied the effects of orbital degeneracy N and doping on the photoemission spectrum in the limit of a large Coulomb interaction U . We find that the degeneracy increases the dispersional width of the spectrum for integer occupancy. Deviations from integer occupancy tends to reduce the width of the spectrum, in particular if the occupation is slightly larger than integer. These effects are gradually reduced as U is reduced or as multiplet effects are taken into account. We also find that the degeneracy tends to reduce the contribution to the specific heat from the charge degrees of freedom, as one would expect from the increased dispersion.

An interesting approach for treating correlation effects is the dynamical mean field theory.¹² In this approach the self-energy is assumed to have no wave vector dependence, which is correct for a system with infinite dimension.^{26,27} The present results show that in a Hubbard model with integer occupancy, the orbital degeneracy increases the \mathbf{k} dependence for intermediate to large values of the Coulomb interaction U . This suggests that the dimension where the dynamical mean field theory becomes accurate increases with the orbital degeneracy.

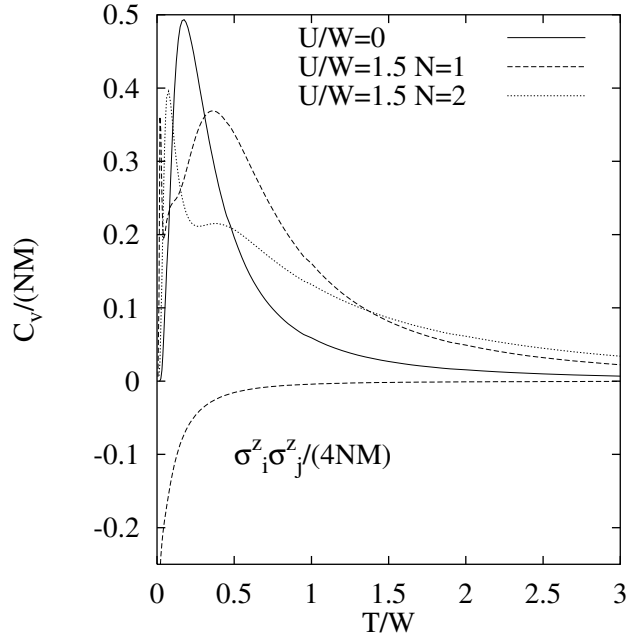


FIG. 14. Specific heat for a six-atom 3×2 cluster with $U/W = 1.5$ as a function of temperature T and degeneracy N . The result for $U = 0$ is also shown. The spin correlation function $\langle \sigma_i^z \sigma_j^z \rangle$ (for $N = 1$) illustrates that the spin degrees of freedom contribute only for small T , while the charge degree of freedoms contribute for larger T . The quantities have been normalized to the number of electrons NM .

It should be emphasized that we have here studied a (degenerate) one-band Hubbard model. For each correlated system one has to consider whether or not this model is appropriate before applying the results above. For certain systems, e.g. heavy fermion and High T_c compounds, the interaction between different types of orbitals plays an important role, and it would be interesting to study how this influences the considerations above.

V. ACKNOWLEDGEMENTS

We would like to thank L.F. Feiner, P. Horsch, E. Koch, R.M. Martin A.M. Oles, and T.M. Rice for stimulating discussions.

¹ S. Hüfner, *Photoelectron Spectroscopy*, Springer Series in Solid-State Sciences 82, Springer, Berlin, 1995.

² S. Hüfner, G.K. Wertheim, N.V. Smith, and M.M. Traum, *Solid State Commun.* **11**, 323 (1972); D.E. Eastman, F.J. Himpsel, and J. A. Knapp, *Phys. Rev. Lett.* **40**, 1514 (1978); H. Mårtensson and P.O. Nilsson, *Phys. Rev. B* **30**, 3047 (1984).

- ³ C.S. Wang and J. Callaway, Phys. Rev. B **15**, 298 (1977).
- ⁴ D.R. Penn, Phys. Rev. Lett. **42**, 921 (1979); A. Liebsch, Phys. Rev. Lett. **43**, 1431 (1979).
- ⁵ J.L. Martins and N. Troullier, Phys. Rev. B **46**, 1766 (1992).
- ⁶ S. Satpathy, V.P. Antropov, O.K. Andersen, O. Jepsen, O. Gunnarsson, and A.I. Liechtenstein, Phys. Rev. B **46**, 177 (1992).
- ⁷ G.J. Burkhardt, and C. Meingast, Phys. Rev. B **54**, R6865 (1996).
- ⁸ F. Aryasetiawan, O. Gunnarsson, E. Koch, and R.M. Martin, Phys. Rev. B **55**, R10165 (1997).
- ⁹ R.W. Lof, M.A. van Veenendaal, B. Koopmans, H.T. Jonkman, and G.A. Sawatzky, 1992, Phys. Rev. Lett. **68**, 3924.
- ¹⁰ O. Gunnarsson, E. Koch, and R.M. Martin, Phys. Rev. B **54**, R11026 (1996).
- ¹¹ O. Gunnarsson, Rev. Mod. Phys. **69**, 575 (1997).
- ¹² See, A. Georges *et al.*, Rev. Mod. Phys. **68**, 13 (1996).
- ¹³ O. Gunnarsson, E. Koch, and R.M. Martin, Phys. Rev. B (in press).
- ¹⁴ E. Koch, O. Gunnarsson, and R.M. Martin (unpublished).
- ¹⁵ V.P. Antropov, O. Gunnarsson, and O. Jepsen, Phys. Rev. B **46**, 13647 (1992).
- ¹⁶ B.N. Parlett, *The symmetric eigenvalue problem*, (Prentice, Englewood, 1980), p. 257.
- ¹⁷ A.B. Harris and R.V. Lange, Phys. Rev. **157**, 295 (1967).
- ¹⁸ W.F. Brinkman and T.M. Rice, Phys. Rev. B **2**, 1324 (1970).
- ¹⁹ See, e.g., K. Penc, K. Hallberg, F. Mila, and H. Shiba, Phys. Rev. Lett. **77**, 1390 (1996) for a recent reference and further references.
- ²⁰ C.T. Chen, T.J. Tjeng, P. Rudolf, G. Meigs, J.E. Rowe, J. Chen, J.P. McCauley Jr., A.B. Smith III, A.R. McGhie, W.J. Romanow, and E.W. Plummer, Nature **352**, 603 (1991).
- ²¹ M. Knupfer, M. Merkel, M.S. Golden, J. Fink, O. Gunnarsson, and V.P. Antropov, Phys. Rev. B **47**, 13944 (1993).
- ²² O. Gunnarsson, S. Satpathy, O. Jepsen, and O.K. Andersen, Phys. Rev. Lett. **67**, 3002 (1991).
- ²³ I.I. Mazin, A.I. Liechtenstein, O. Gunnarsson, O.K. Andersen, V.P. Antropov, and S.E. Burkov, Phys. Rev. Lett. **26**, 4142 (1993).
- ²⁴ E. Antonides, E.C. Janse, and G.A. Sawatzky, Phys. Rev. B **15**, 1669 (1977).
- ²⁵ J. Jaklic and P. Prelovsek, Phys. Rev. B **49**, 5065 (1994).
- ²⁶ W. Metzner and D. Vollhardt, Phys. Rev. Lett. **62**, 324 (1989).
- ²⁷ E. Müller-Hartmann, Z. Phys. B **74**, 507 (1989).